Towards Higher Alcohol Formation using a single-layer MoS_2 activated Au on Silica: Methanol Carbonylation to Acetaldehyde

Kortney Almeida,[1] Katerina L. Chagoya,[2] Alan Felix,[2] Tao Jiang,[3] Duy Le,[3] Takat B. Rawal,[4] Prescott E. Evans,[5] Michelle Wurch,[1] Koichi Yamaguchi,[1] Peter A. Dowben,[5] Ludwig Bartels,[1,*] Talat S. Rahman,[3,*] Richard G. Blair[6,*]

[1] *Department of Chemistry and Materials Science & Engineering Program, University of California - Riverside, Riverside, CA 92521, U.S.A.*

[2] *Department of Mechanical and Aerospace Engineering, University of Central Florida, 12760 Pegasus Dr., Orlando, FL 32816, U.S.A.*

[3] *Department of Physics, University of Central Florida, 4111 Libra Drive, Orlando, FL 32816, U.S.A.*

[4] *UT/ORNL Center for Molecular Biophysics, Oak Ridge National Laboratory, Oak Ridge, TN, 37830, U.S.A.*

[5] *Department of Physics and Astronomy, Theodore Jorgensen Hall, 855 N 16th, University of Nebraska, Lincoln, NE 68588-0299, U.S.A.*

[6] *Florida Space Institute, University of Central Florida, 12354 Research Parkway, Suite 214, Orlando, U.S.A.*

*Corresponding Author Email:*bartels@ucr.edu, talat@ucf.edu, *and* Richard.Blair@ucf.edu

Abstract

We demonstrate that a fused silica substrate can be rendered active for acetaldehyde (CH_3CHO) synthesis from a gas mixture of carbon monoxide (CO) and methanol (CH_3OH) under mild process conditions (308 kPa and 393 K) by deposition first of a homogenous single-layer MoS_2 film and subsequently of a sub-mnonolayer (1 Angstrom) loading of gold. *In operando* monitoring of the catalyst performance in a flow reactor reveals uncompromised activity even after 2 hours on stream. The carbonylation of methanol to a C_2 species represents a crucial step toward the formation of higher alcohols from syngas derived from methane or biomass. Characterization of the film by imaging and spectroscopy reveals that the single-layer MoS_2 film disperses the gold loading into nanoscale islands; density functional theory (DFT) calculations identify low-coordinated edge sites on these islands as active centers for the carbon-carbon coupling at barriers significantly below 1 eV.

.

Introduction

The formation of higher alcohols from syngas is an important goal in the quest for economic and sustainable transformation of biomass into transportation fuels. A necessary step for its realization is efficient C-C coupling involving oxygenate small molecules such as carbon monoxide and methanol. The seminal finding by Haruta of CO oxidation by supported nanoscale gold particles[1] showed that gold, despite being arguably the most noble of metals,[2] can play an active role in heterogeneous catalysis. In recent work,[3-5] we have shown that single-layer MoS_2 coating can transform an otherwise inert substrate, silica, into a catalytic active surface for e.g. CO oxidation by gold nanoclusters, similar to results obtained for reducible oxides, such as titania and ceria.[6-12] Concomitant computational efforts have predicted a number of feasible, low-barrier reaction pathways on thus supported gold nanoparticles,[3, 13] in contrast to the largely catalytically inactive bulk gold, Au on pristine silica or on other 2D materials like graphene.[14-16] Here, we address the carbonylation of methanol as the most fundamental C-C coupling step that can lead to higher alcohol formation from a lower alcohol and a component of syngas, as it may be obtained from biomass gasification.

A wide range of catalytic applications have been proposed for MoS_2, both in the past and more recently. MoS_2 with cobalt and alkali modifiers is the key catalyst material in industrial hydrodesulfurization; notably, the industrial catalyst material resembles a few-layer film.[17] MoS_2 modified by alkali has also been proposed for alcohol formation.[18-26] The mechanistic aspects of these studies by and large focus on the hydrogenation step, in particular the initial CO hydrogenation. In contrast, our study focusses on the extension of the carbon chain (Fig. 1a) toward higher alcohols by means of carbonylation of methanol.

MoS_2 has gained prominence as a catalyst for hydrogen evolution;[27, 28] its activity has been attributed to edge sites based on low-temperature measurements,[29] and related materials that feature large number of exposed edge sites have been prepared and validated in some catalytic applications.[30-36] We have avoided such complications by developing a process that provides pristine single-layer MoS_2 coatings over several centimeter in diameter.[37]

In this work, the formation of acetaldehyde at reactor temperatures as low as 393 K, on single layer MoS_2 films, decorated by nanoscale gold islands, is evident using a plug flow reactor system with on process gas chromatography. Density functional theory (DFT) modeling sheds light on the crucial carbon-carbon coupling step at the center of this finding.

Experimental

We inserted a stream of CO bubbled through methanol into a continues flow reactor equipped with a Ø1.5 cm fused silica window coated homogeneously with precisely a single layer of MoS_2 decorated by nanoscale gold islands corresponding to an average gold coverage of 1Å or ~ 1/3 of a monolayer Figure 1b shows the preparative effort schematically and Fig. 1c depicts the fused silica window after single-layer MoS_2 and gold deposition.

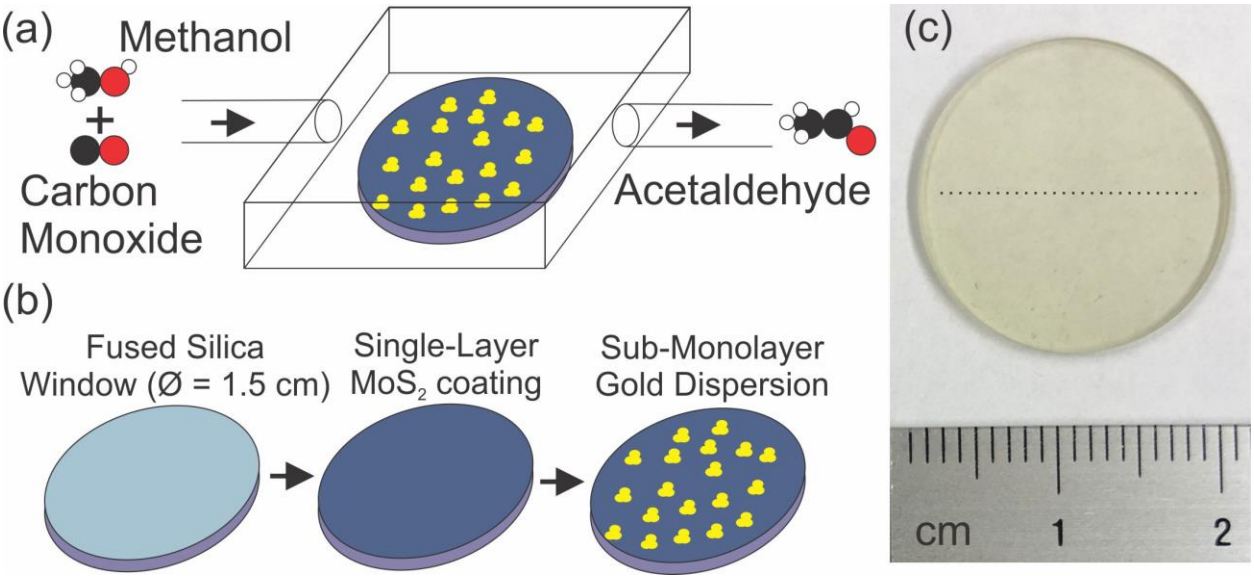

Fig. 1: *a,b) Schematic representation of the catalyst preparation and the experimental process; c) photograph of the Ø1.5 cm fused silica window coated with a single-layer of* MoS_2 *and deposition of gold.*

To make the catalysis, we have exploited a technique for coating of inert oxides by an MoS_2 films of controlled integer layer number, as reported elsewhere.[37] This earlier work[37] focused on MoS_2 films on a dry oxide SiO_2 layer on a silicon wafer substrate. This MoS_2 growth technique is based on heating molybdenum filaments to white glow (>1500 K) under high vacuum followed by exposure to carbon disulfide. Decomposition of the disulfide on the Mo filament surface results in volatile MoS_x precursors, which are precipitated on the substrate held at a temperature that affords an equilibrium of MoS_2 island growth and desorption. The growth is monitored via the hue of the reflection of the filament on a small 300 nm SiO_2/Si reference substrate processed along with the fused silica window; the deposition is terminated when the hue reaches the characteristic value of a single-layer film. In order to apply scanning electron microscopy imaging to ascertain the nanoscale nature of the gold cluster, we also prepared a sample on a thin (30 nm) silicon dioxide film on a doped silicon substrate. Gold deposition used

an e-beam evaporator and a quartz crystal microbalance; deposition proceeded at a rate of a fraction of an Ångstrom per minute.

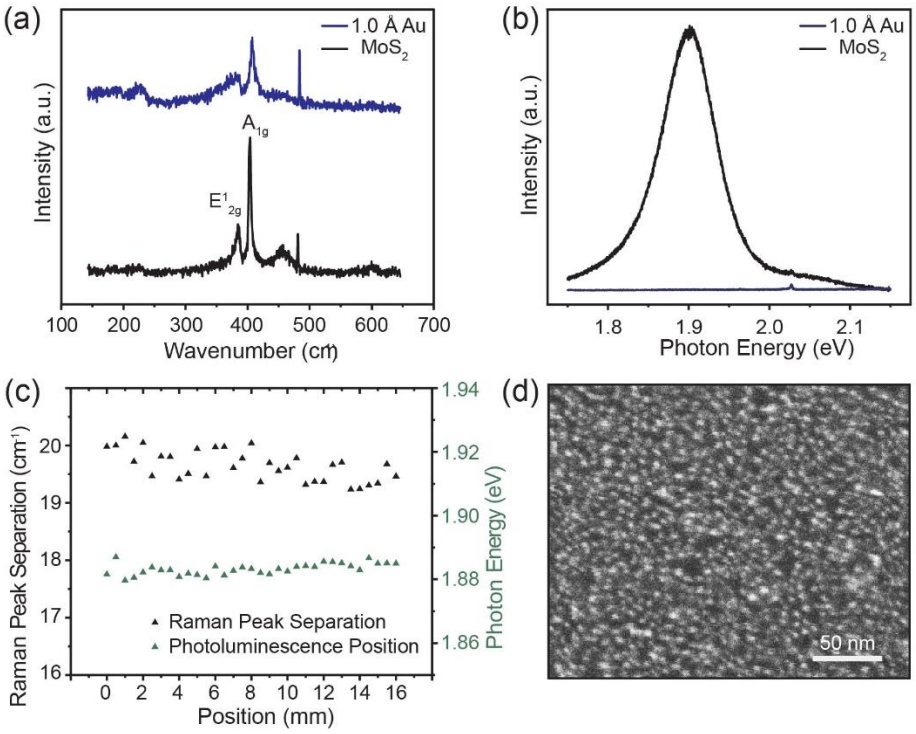

Fig. 2 *The (a) Raman and (b) photoluminescence spectra of a single-layer MoS_2 sample before (black) and (blue) after sub-monolayer gold deposition; (c) homogeneity of single-layer MoS_2 film across the fused silica substrate: Raman A_{1g} - E_{2g} peak separation and photoluminescence position were mapped along the dashed horizontal line of Fig. 1c. (d) SEM image of Au dispersion across the top of a single layer MoS_2 film on a 30nm silica test film. A homogeneous distribution of gold clusters each smaller than a few nanometers is observed.*

The MoS_2 samples are single layer, as seen in Figure 2: we find the typical Raman peak positions for single-layer MoS_2 films for E_{2g} and A_{1g} modes at 385.5 cm^{-1} and 404.9 cm^{-1} (separation 19

cm^{-1});[38] Gold deposition broadens the modes. Before gold deposition, the photoluminescence of the substrate material was bright and centered at 1.91 eV with a full-width at half-maximum ~0.1 eV, the well-established optical bandgap of single-layer MoS_2.[39, 40] After gold deposition, the photoluminescence is quenched. This indicates that despite the small gold dosage of only 1/3 of a monolayer there is a quenching center within the size of practically any exciton created on the surface. This corroborates efficient dispersion of gold on MoS_2/SiO_2, much in contrast to gold on bare silica or graphene. Direct scanning electron microscopy (SEM) imaging of a test sample with a 30nm silica film on silicon shows tiny, point-like gold particles below the limit of the instrument for resolution of internal features. These particles are 1-3 nanometers in size at maximum, i.e. in the crucial size range for catalytic activity.[41-43]

Reactor studies were performed on a plug flow reactor; for product separation we employed two gas chromatographs: An Agilent 6890 with a crossbond dimethylsiloxane column (Restek RTX-1, 30 m, 0.25 mm ID, 0.5 µm film thickness) and a mass sensitive detector (Agilent 5973) was utilized for samples taken with a 25 mL gas tight syringe from a sampling port in the product stream. An Agilent 6850 with a thermal conductivity detector (TCD) was connected directly to the product stream via a transfer line and a gas sampling valve. Chromatographic methods and the plug flow reactor are further described in the supplementary material.

Acetaldehyde Production

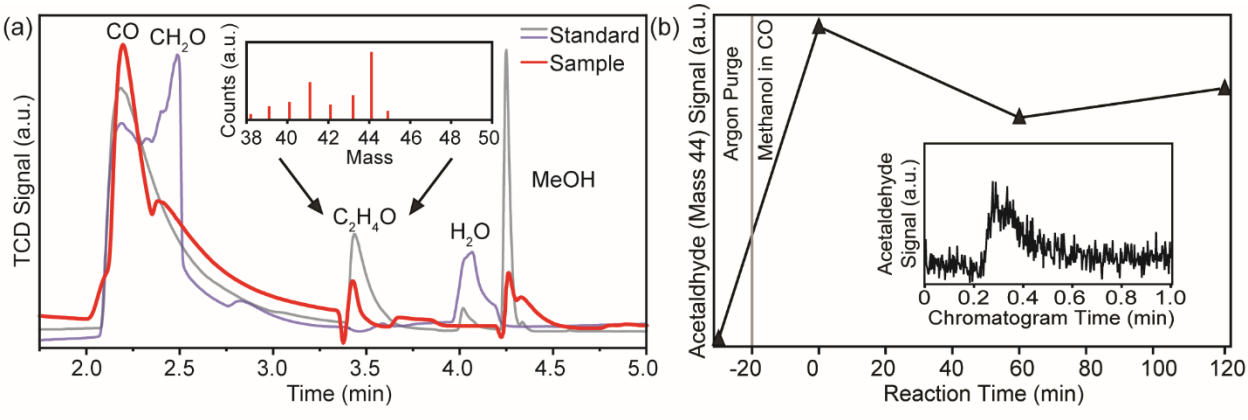

Fig. 3 *The (a) Gas chromatograms using thermocouple detection of the flow reactor output and two standard analytes as labeled. The double peaks in the reactor output are caused by the sampling valve. The inset shows the fragmentation pattern of the acetaldehyde peak using mass spectrometric detection. (b) Integrated acetaldehyde peak intensity using mass spectrometric detection as a function of the on-stream time of the catalyst shows sustained activity even after 120 min. The inset shows the acetaldehyde peak observed at 60 min into the reaction.*

As reactant we used CO gas bubbled through a reservoir of methanol at 20 °C and 308 kPa resulting in a methanol vapor concentration of 4.2% in the feed stream. Prior to the reaction, the reactor was purged with argon gas and heated to the reaction temperature of 120°C. Fig. 3a compares a chromatogram obtained at 60 minutes after starting a catalytic experiment with two standard analytes, one containing CO, water, acetaldehyde and methanol, and the other CO, formaldehyde and water. Note, that the shoulder on the sampling peaks are caused by incomplete closing of the sampling valve and are not indicative of impurities. Comparison of the chromatogram with the standard analytes reveals that the reactor product stream contains not only the reactants (CO and methanol) but also acetaldehyde. While no water was detected, we

cannot rule out a small amount of water production and condensation in the transfer lines (which are not heated in our setup). The mass spectrogram insert shows the fragmentation pattern of the acetaldehyde peak, thus ascertaining the chemical assignment.

We explored the stability of the catalyst by running the reactor for 2 hours. Fig. 3b shows the production of acetaldehyde as time on stream. While we observe a slight drop initially, we find that subsequently the reaction proceeds at near-constant rate. This attests to the long-term stability of our catalyst composition and rules out that conversion of impurities in a non-catalytic fashion are responsible for the production of acetaldehyde.

In order to determine the origin of the observed reactivity, we also explored the same reaction using bulk MoS_2 decorated with 1 Angstrom of gold as a substrate. We do not observe the formation of acetaldehyde on these samples. This finding clearly points to the importance of the single layer film for activating the gold nanoparticles, as has been reported prior by some of us.

Density functional theory-based calculations

Accompanying density functional theory (DFT) calculations validate the feasibility of the formation of carbon-carbon bonds at the surface of MoS_2-supported Au nanoparticles and illuminate the underlying elementary reactions steps. Continuing the success of previous computational work,[3-5] in which the alcohol synthesis from syngas (CO and H_2) was shown to be feasible on Au_{13} nanoparticles stabilized by interactions with a single layer of MoS_2, we use the same supercell setup to study the formation of a bond between adsorbed methyl and carbonyl species to acetyl (Fig. 4a) and subsequent hydrogenation to acetaldehyde (Fig. 4b) followed by

desorption: (I) CH_3* + CO* → CH_3CO* and (II) CH_3CO* + H* → CH_3CHO* (* indicates adsorbed species).

The reactant CH_3* and H* are the products of methanol dissociative adsorption followed by formation of CO_2 by reaction of O* with CO* as described elsewhere.[5] Details of calculations can be found in Ref [[3]]. Fig. 4a,b shows the initial state, transition state, and final states of the CH_3* + CO* → CH_3CO* and CH_3CO* + H* → CH_3CHO* reactions. Our calculations indicate that the formation of a bond between the adsorbed CH_3* species and a CO* molecule on Au_{13} is well feasible as the reactions are exothermic and the activation barriers comparatively low: 0.69 eV for the acetyl formation (I) (Fig. 4a) and 0.47 eV for the hydrogenation of acetyl to acetaldehyde (II) (Fig 4b). The resultant CH_3CHO* is found to desorb to the gas phase with a desorption energy of 0.45 eV.

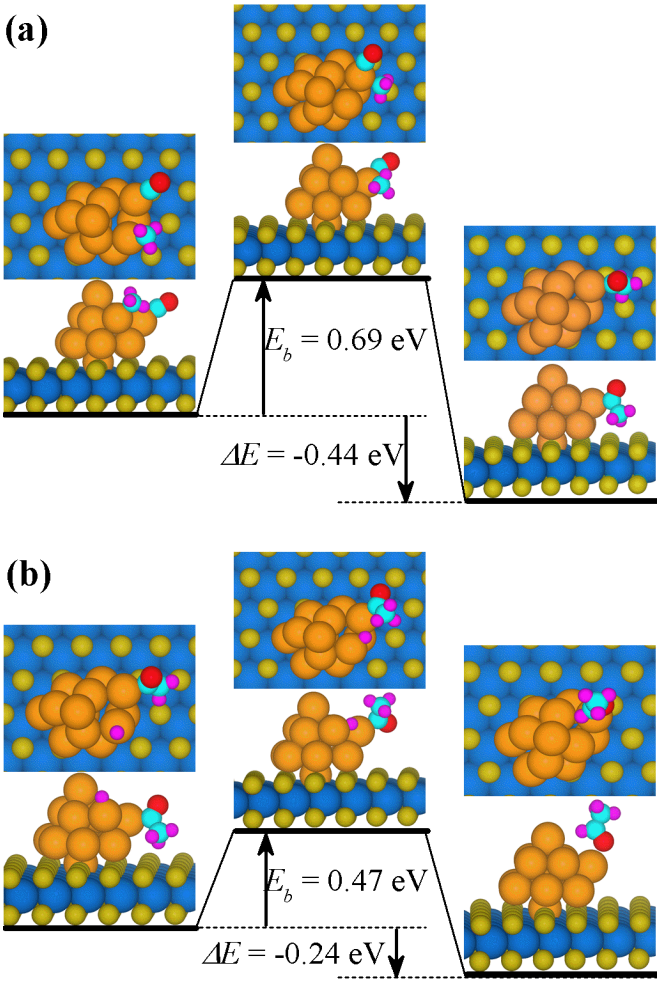

Fig. 4: Reaction pathways of CH_3 + CO* → CH_3CO* (a) and CH_3CO* + H* → CH_3CHO* (b). Left, central, and right cartoons show both top and side views of initial, transition, and final states, respectively. Blue, yellow, gold, cyan, red, and magenta balls represent Mo, S, Au, C, O, and H atoms, respectively. E_b and ΔE are activation barrier and reaction energy, respectively.*

The adsorption sites and reaction pathways, shown in Fig. 4, is the result from a wide search for the lowest barrier pathway on these clusters. Close inspection reveals that site with the lowest barriers corresponds to the least coordinated gold atom on the cluster, where the binding of the reactants is strongest. This finding highlights the importance of small clusters for this reaction to proceed. Such sites are far more common on small gold clusters compared to larger ones. Thus,

the ability of even a single-layer of MoS_2 to disperse gold into nanometer-scale clusters[13] is at the root of the availability of this reaction pathway in the system at hand.

Conclusion

The deposition of gold nanoparticles on a single layer of MoS_2 on an inert fused silica substrate provides a surface capable of upconverting methanol to acetaldehyde. Our findings highlight an important first step towards the formation of longer alcohols from methanol or even syngas using inexpensive, non-toxic, earth-abundant MoS_2 and less than a monolayer of gold. This new finding is an exciting milestone for good reasons as it showcases the promise of gold nanoparticles on a single layer of MoS_2. The low reaction temperatures and pressures (120 °C and ~3 atm) further support the appeal of this approach. Additionally, acetaldehyde can be oxidized to acetic acid yielding a route to acetic acid without the need for iodides. The basal plane of MoS_2 is inert, yet the material is a well-established catalyst for hydrodesulfurization and -denitrogenation, though reasons for the reactivity have thus far been elusive. Our results illustrate a mechanism by which single-layer MoS_2 can indeed be activated. Furthermore, our results also speak to sustained reactivity of Au nanoparticles in a scenario in which inert substrates can be first shaped into desired structures that optimize reactant and heat flow and serve as an inexpensive scaffold for a composite that bestows catalytic activity on them.

Supporting Information

Supporting information is available: reactor setup, chromatographic methods

Acknowledgements

We gratefully acknowledge joint funding from the US Department of Energy grant DE-FG02-07ER15842 (UCF, UCR, UNL). We thank the Advanced Research Computing Center at the University of Central Florida, and the National Energy Research Scientific Computing Center (NERSC) for providing the computer resources.

References

1. Haruta, M.; Kobayashi, T.; Sano, H.; Yamada, N., Novel Gold Catalysts for the Oxidation of Carbon-Monoxide at a Temperature Far Below 0-Degrees-C. *Chem. Lett.* **1987**, (2), 405-408.
2. Hammer, B.; Norskov, J. K., Why gold Is the noblest of all the metals. *Nature* **1995,** 376, (6537), 238-240.
3. Rawal, T. B.; Le, D.; Rahman, T. S., Effect of single-layer MoS_2 on the geometry, electronic structure, and reactivity of transition metal nanoparticles. *J. Phys. Chem. C* **2017,** 121, (13), 7282-7293.
4. Rawal, T. B.; Le, D.; Rahman, T. S., MoS_2–supported gold nanoparticle for CO hydrogenation. *Journal of Physics: Condensed Matter* **2017, 29**, (41), 415201.
5. Almeida, K.; Pena, P.; Rawal, T. B.; Coley, W. C.; Akhavi, A.-A.; Wurch, M.; Yamaguchi, K.; Le, D.; Rahman, T. S.; Bartels, L., A Single-Layer of MoS_2 activates Gold for Room Temperature CO Oxidation on an Inert Silica Substrate. *J. Phys. Chem. C* **2019,** 123 (11), 6592–6598.
6. Haruta, M.; Tsubota, S.; Kobayashi, T.; Kageyama, H.; Genet, M. J.; Delmon, B., Low-temperature oxidation of CO over gold supported on TiO_2, alpha-Fe_2O_3, and Co_3O_4. *J. Catal.* **1993,** 144, (1), 175-192.
7. Schubert, M. M.; Plzak, V.; Garche, J.; Behm, R. J., Activity, selectivity, and long-term stability of different metal oxide supported gold catalysts for the preferential CO oxidation in H-2-rich gas. *Catal. Lett.* **2001,** 76, (3-4), 143-150.
8. Deng, W. L.; De Jesus, J.; Saltsburg, H.; Flytzani-Stephanopoulos, M., Low-content gold-ceria catalysts for the water-gas shift and preferential CO oxidation reactions. *Applied Catalysis* **2005,** A291, (1-2), 126-135.
9. Gardner, S. D.; Hoflund, G. B.; Schryer, D. R.; Schryer, J.; Upchurch, B. T.; Kielin, E. J., Catalytic Behavior of Noble-Metal Reducible Oxide Materials for Low-Temperature Co Oxidation .1. Comparison of Catalyst Performance. *Langmuir* **1991,** 7, (10), 2135-2139.
10. Chen, M. S.; Goodman, D. W., The structure of catalytically active gold on titania. *Science* **2004,** 306, (5694), 252-255.
11. Zhou, Y. Y.; Lawrence, N. J.; Wang, L.; Kong, L. M.; Wu, T. S.; Liu, J.; Gao, Y.; Brewer, J. R.; Lawrence, V. K.; Sabirianov, R. F.; Soo, Y. L.; Zeng, X. C.; Dowben, P. A.; Mei, W. N.; Cheung, C. L., Resonant Photoemission Observations and DFT Study of s-d Hybridization in Catalytically Active Gold Clusters on Ceria Nanorods. *Angew. Chem. Int. Ed. Engl.* **2013,** 52, (27), 6936-6939.

12. Yang, F.; Graciani, J.; Evans, J.; Liu, P.; Hrbek, J.; Sanz, J. F.; Rodriguez, J. A., CO Oxidation on Inverse CeO(x)/Cu(111) Catalysts: High Catalytic Activity and Ceria-Promoted Dissociation of O(2). *J. Am. Chem. Soc.* **2011,** 133, (10), 3444-3451.
13. Merida, C. S.; Le, D.; Echeverria, E. M.; Nguyen, A. E.; Rawal, T. B.; Alvillar, S. N.; Kandyba, V.; Al-Mahboob, A.; Losovyj, Y.; Katsiev, K.; Valentin, M. D.; Huang, C. Y.; Gomez, M. J.; Lu, I. H.; Guan, A.; Barinov, A.; Rahman, T. S.; Dowben, P. A.; Bartels, L., Gold Dispersion and Activation on the Basal Plane of Single-Layer MoS_2. *J. Phys. Chem. C* **2018,** 122, (1), 267-273.
14. Wang, B.; Bocquet, M. L., Monolayer Graphene and h-BN on Metal Substrates as Versatile Templates for Metallic Nanoclusters. *J. Phys. Chem. Lett.* **2011,** 2, (18), 2341-2345.
15. Katsiev, K.; Losovyj, Y.; Lozova, N.; Wang, L.; Mei, W. N.; Zheng, J. X.; Vescovo, E.; Liu, L.; Dowben, P. A.; Goodman, D. W., The band structure of carbonmonoxide on 2-D Au islands on graphene. *Appl. Surf. Sci.* **2014,** 304, 35-39.
16. Zheng, J. X.; Wang, L.; Katsiev, K.; Losovyj, Y.; Vescovo, E.; Goodman, D. W.; Dowben, P. A.; Lu, J.; Mei, W. N., Adsorption configurations of carbon monoxide on gold monolayer supported by graphene or monolayer hexagonal boron nitride: a first-principles study. *Eur. Phys. J. B* **2013,** 86, (10).
17. Hansen, L. P.; Ramasse, Q. M.; Kisielowski, C.; Brorson, M.; Johnson, E.; Topsoe, H.; Helveg, S., Atomic-scale edge structures on industrial-style MoS_2 nanocatalysts. *Angew. Chem. Int. Ed. Engl.* **2011,** 50, (43), 10153-10156.
18. Surisetty, V. R.; Dalai, A. K.; Kozinski, J., Alcohols as alternative fuels: An overview. *Appl. Catal., A* **2011,** 404, (1-2), 1–11.
19. Morrill, M. R.; Thao, N. T.; Shou, H.; Davis, R. J.; Barton, D. G.; Ferrari, D.; Agrawal, P. K.; Jones, C. W., Origins of Unusual Alcohol Selectivities over Mixed Mg Al Oxide-Supported K/MoS_2 Catalysts for Higher Alcohol Synthesis from Syngas. *Acs Catalysis* **2013,** 3, (7), 1665-1675.
20. Claure, M. T.; Chai, S. H.; Dai, S.; Unocic, K. A.; Alamgir, F. M.; Agrawal, P. K.; Jones, C. W., Tuning of higher alcohol selectivity and productivity in CO hydrogenation reactions over K/MoS_2 domains supported on mesoporous activated carbon and mixed MgAl oxide. *J. Catal.* **2015,** 324, 88-97.
21. Surisetty, V. R.; Dalai, A. K.; Kozinski, J., Synthesis of higher alcohols from synthesis gas over Co-promoted alkali-modified MoS_2 catalysts supported on MWCNTs. *Appl. Catal. A-Gen.* **2010,** 385, (1-2), 153-162.
22. Lv, M. M.; Xie, W.; Sun, S.; Wu, G. M.; Zheng, L. R.; Chu, S. Q.; Gao, C.; Bao, J., Activated-carbon-supported K-Co-Mo catalysts for synthesis of higher alcohols from syngas. *Catalysis Science & Technology* **2015,** 5, (5), 2925-2934.
23. Xie, W.; Zhou, J. L.; Ji, L. L.; Sun, S.; Pan, H. B.; Zhu, J. F.; Gao, C.; Bao, J., Targeted design and synthesis of a highly selective Mo-based catalyst for the synthesis of higher alcohols. *Rsc Advances* **2016,** 6, (45), 38741-38745.
24. Luk, H. T.; Mondelli, C.; Ferre, D. C.; Stewart, J. A.; Perez-Ramirez, J., Status and prospects in higher alcohols synthesis from syngas. *Chemical Society Reviews* **2017,** 46, (5), 1358-1426.
25. Luk, H. T.; Forster, T.; Mondelli, C.; Siol, S.; Curulla-Ferre, D.; Stewart, J. A.; Perez-Ramirez, J., Carbon nanofibres-supported KCoMo catalysts for syngas conversion into higher alcohols. *Catalysis Science & Technology* **2018,** 8, (1), 187-200.
26. Ao, M.; Pham, G. H.; Sunarso, J.; Tade, M. O.; Liu, S. M., Active Centers of Catalysts for Higher Alcohol Synthesis from Syngas: A Review. *Acs Catalysis* **2018,** 8, (8), 7025-7050.
27. Kim, J.; Byun, S.; Smith, A. J.; Yu, J.; Huang, J. X., Enhanced electrocatalytic properties of transition-metal dichalcogenides sheets by spontaneous gold nanoparticle decoration. *J. Phys. Chem. Lett.* **2013,** 4, (8), 1227-1232.
28. Osaki, T.; Narita, N.; Horiuchi, T.; Sugiyama, T.; Masuda, H.; Suzuki, K., Kinetics of reverse water gas shift (RWGS) reaction on metal disulfide catalysts. *J. Mol. Catal. A: Chem.* **1997,** 125, (1), 63-71.

29. Besenbacher, F.; Brorson, M.; Clausen, B. S.; Helveg, S.; Hinnemann, B.; Kibsgaard, J.; Lauritsen, J.; Moses, P. G.; Norskov, J. K.; Topsoe, H., Recent STM, DFT and HAADF-STEM studies of sulfide-based hydrotreating catalysts: Insight into mechanistic, structural and particle size effects. *Catal. Today* **2008,** 130, (1), 86-96.
30. Sun, D.; Lu, W.; Le, D.; Ma, Q.; Aminpour, M.; Alcántara Ortigoza, M.; Bobek, S.; Mann, J.; Wyrick, J.; Rahman, T. S.; Bartels, L., An MoS_x Structure with High Affinity for Adsorbate Interaction. *Angewandte Chemie* **2012,** 124, (41), 10430-10434.
31. Kibsgaard, J.; Chen, Z. B.; Reinecke, B. N.; Jaramillo, T. F., Engineering the surface structure of MoS2 to preferentially expose active edge sites for electrocatalysis. *Nat. Mater.* **2012,** 11, (11), 963-969.
32. Ho, T. A.; Bae, C.; Lee, S.; Kim, M.; Montero-Moreno, J. M.; Park, J. H.; Shin, H., Edge-On MoS2 Thin Films by Atomic Layer Deposition for Understanding the Interplay between the Active Area and Hydrogen Evolution Reaction. *Chem Mater* **2017,** 29, (17), 7604-7614.
33. Ma, Q.; Odenthal, P. M.; Mann, J.; Le, D.; Wang, C. S.; Zhu, Y. M.; Chen, T. Y.; Sun, D. Z.; Yamaguchi, K.; Tran, T.; Wurch, M.; McKinley, J. L.; Wyrick, J.; Magnone, K.; Heinz, T. F.; Rahman, T. S.; Kawakami, R.; Bartels, L., Controlled argon beam-induced desulfurization of monolayer molybdenum disulfide. *J. Phys.-Condens. Mat.* **2013,** 25, (25), 252201.
34. Ma, Q.; Isarraraz, M.; wang, C.; Preciado, E.; Klee, V.; Bobek, S.; Yamaguchi, K.; li, E.; Odenthal, P. M.; nguyen, A.; Barroso, D.; Sun, D.; Palacio, G. V.; Gomez, M.; nguyen, A.; Le, D.; Pawin, G.; mann, J.; Heinz, T. F.; Rahman, T.; Bartels, L., Postgrowth tuning of the bandgap of single-layer molybdenum disulfide films by sulfur/selenium exchange. *ACS Nano* **2014,** 8, (5), 4672-4677.
35. Le, D.; Rawal, T. B.; Rahman, T. S., Single-Layer MoS2 with Sulfur Vacancies: Structure and Catalytic Application. *J. Phys. Chem. C* **2014,** 118, (10), 5346-5351.
36. Le, D.; Rahman, T. S., Joined edges in MoS2: metallic and half-metallic wires. *J. Phys.-Condens. Mat.* **2013,** 25, (31).
37. Almeida, K.; Wurch, M.; Geremew, A.; Yamaguchi, K.; Empante, T. A.; Valentin, M. D.; Gomez, M.; Berges, A. J.; Stecklein, G.; Rumyantsev, S.; Martinez, J.; Balandin, A. A.; Bartels, L., High-Vacuum Particulate-Free Deposition of Wafer-Scale Mono-, Bi-, and Trilayer Molybdenum Disulfide with Superior Transport Properties. *ACS Appl Mater Interfaces* **2018,** 10, (39), 33457-33463.
38. Lee, C.; Yan, H.; Brus, L. E.; Heinz, T. F.; Hone, J.; Ryu, S., Anomalous Lattice Vibrations of Single- and Few-Layer MoS_2 *ACS Nano* **2010,** 4, (5), 2695-2700.
39. Mak, K. F.; Lee, C.; Hone, J.; Shan, J.; Heinz, T. F., Atomically thin MoS_2: a new direct-gap semiconductor. *Phys. Rev. Lett.* **2010,** 105, (13), 136805.
40. Splendiani, A.; Sun, L.; Zhang, Y. B.; Li, T. S.; Kim, J.; Chim, C. Y.; Galli, G.; Wang, F., Emerging photoluminescence in monolayer MoS_2 *Nano Lett.* **2010,** 10, (4), 1271-1275.
41. Valden, M.; Lai, X.; Goodman, D. W., Onset of catalytic activity of gold clusters on titania with the appearance of nonmetallic properties. *Science* **1998,** 281, (5383), 1647-1650.
42. Lopez, N.; Janssens, T. V. W.; Clausen, B. S.; Xu, Y.; Mavrikakis, M.; Bligaard, T.; Norskov, J. K., On the origin of the catalytic activity of gold nanoparticles for low-temperature CO oxidation. *J. Catal.* **2004,** 223, (1), 232-235.
43. Bondzie, V. A.; Parker, S. C.; Campbell, C. T., The kinetics of CO oxidation by adsorbed oxygen on well-defined gold particles on TiO2(110). *Catal. Lett.* **1999,** 63, (3-4), 143-151.